MEDICAL SCIENCE MONITOR

CLINICAL RESEARCH

e-ISSN 1643-3750
© Med Sci Monit, 2024; 30: e943705
DOI: 10.12659/MSM.943705

Received: 2024.01.04
Accepted: 2024.02.28
Available online: 2024.03.26
Published: 2024.XX.XX

New Computerized Planning Algorithm and Clinical Testing of Optimized Nuss Bar Design for Patients with Pectus Excavatum

Authors' Contribution:
Study Design A
Data Collection B
Statistical Analysis C
Data Interpretation D
Manuscript Preparation E
Literature Search F
Funds Collection G

ABCDEF 1 János György Papp
B 1 Ákos Kiss
BC 2 Krisztián Balogh
BC 2 László Kostyál
BC 3 Imre Tóth
BCD 4 Tibor Gáll
DEF 5 Péter Vajda
DEF 6 Tamás F. Molnár
CD 7 István Papp
EF 8,9 László Szabó
ACDEF 10 Árpád B. Palotás

1 Department of Pediatric Surgery, Traumatology and Burns, Borsod-Abaúj-Zemplén County Hospital and University Teaching Hospital (BKEOK), Miskolc, Hungary
2 Institute of Radiology, Borsod-Abaúj-Zemplén County Hospital and University Teaching Hospital (BKEOK), Miskolc, Hungary
3 Department of Thoracic Surgery, Borsod-Abaúj-Zemplén County Hospital and University Teaching Hospital (BKEOK), Miskolc, Hungary
4 Institute of Public Health and Epidemics, University of Debrecen Medical School, Debrecen, Hungary
5 Department of Pediatrics, Division of Pediatric Surgery, University of Pécs, Medical School, Pécs, Hungary
6 Department of Operational Medicine, University of Pécs, Medical School, Pécs, Hungary
7 Senior Software Developer, Budapest, Hungary
8 Department of Family Care Methodology, Semmelweis University, Budapest, Hungary
9 Heim Pál National Pediatric Institute, Budapest, Hungary
10 Faculty of Materials & Chemical Engineering, University of Miskolc, Miskolc, Hungary

Corresponding Authors: János György Papp, e-mail: drpaja.mail@gmail.com; Péter Vajda, e-mail: peter.vajda@aok.pte.hu, Tamás F. Molnár, e-mail: tfmolnar@gmail.com, Árpád B. Palotás, e-mail: arpad.palotas@uni-miskolc.hu

Financial support: None declared
Conflict of interest: None declared

Background: Computer-aided design (CAD) has been used in the Nuss procedure to determine the bar length and shape. Despite computer aid, the shape and design remain quite intuitive. We tested a new algorithm to determine the optimal bar shape.

Material/Methods: The normal sterno-vertebral distance was defined on computed tomography (CT) scans of patients without pectus excavatum (PEx) at the same level where the deepest depression was found on CT scans of 97 patients with PEx. Four points were marked on the CT scan of 60 patients with PEx at the deepest deformity: P1: edge of the vertebra; P2: edge of the deformity; P3: the expected contact point of the bar and the rib; and P4: the expected end of the bar. The algorithm generated 3 circles upon these points, and the fusion of the arcs drew the line of the ideal bar. Corrected and normal sterno-vertebral distance values were compared with the Mann-Whitney U test. Ten bars were bent manually guided by a 1: 1 printout of the designed bar and were implanted in 10 adolescents.

Results: The shortest sterno-vertebral distance was 3 cm below the intermammillary line in PEx patients. The normal mean sterno-vertebral distance at this level was 10.16±1.35 cm in non-PEx patients. The mean virtually corrected sterno-vertebral distance was 10.28±1.27 cm. No significant difference was found (P=0.44). The bars were seamless and were successfully implanted. No bar needed adjustment, the operation time was shorter, and the patient satisfaction score was 9.4/10.

Conclusions: With our new algorithm, an optimal Nuss bar can be designed.

Keywords: **Pectus Excavatum • Nuss Procedure • Computer-Aided Design of Custom-Made Nuss Bar • Python Software • Mathematical Model • Thoracic Deformity • CT-Based Geometric Correction Algorithm • Individual Implant**

Abbreviations: **PEx** – pectus excavatum; **CT** – computer tomography; **CAD** – computer-aided design

Full-text PDF: https://www.medscimonit.com/abstract/index/idArt/943705

3261 4 7 19

Indexed in: [Current Contents/Clinical Medicine] [SCI Expanded] [ISI Alerting System] [ISI Journals Master List] [Index Medicus/MEDLINE] [EMBASE/Excerpta Medica] [Chemical Abstracts/CAS]

Introduction

Pectus excavatum (PEx) is the most common anterior chest wall deformity. The deformity can be mild, with a Haller index <3.2, or more severe, with a Haller index >3.2 [1]. The more severe deformities can affect cardiac and pulmonary functions [2-6]. Although the less severe deformity can be considered "only a cosmetic issue", it can have a detrimental psychologic effect on adolescents; therefore, there is a significant demand for treatment, and in many countries, treatment is still paid by national insurance plans. Conservative management with the vacuum bell is successful in only mild deformities and requires significant patience and compliance, which teenagers often lack [7]. The surgical management of PEx changed significantly the last 2 decades. The Nuss procedure [8,9] replaced the more difficult and invasive Ravitch procedure [10]. The newest extracorporal traction technique (pectus up) [11,12] seems very promising; however, there are no sufficient clinical data available on the outcomes, and the equipment is complicated and expensive. The initial concern regarding cardiac injury with the Nuss procedure was significantly reduced with the application of thoracoscopy. (The authors performed over 600 procedures without major complication the last 20 years.) The growing experience of surgeons can make the Nuss procedure the criterion standard surgical option for management of PEx.

During the Nuss procedure, the bars are to be bent manually by the surgeons to the desired shape. This is still a challenging and time-consuming procedure. If the bar is not bent to the ideal shape the first time, it will need to be removed, adjusted, and reintroduced to achieve an optimal outcome; however, this increases the operative time and the risk of complications and injuries.

The preoperative customization of the bar is not a new idea. Computer-aided design (CAD), finite element analysis, computer-aided manufacturing (3D printing or computer-aided bending [computer numerical computing] of the bar) simulated surgery on a 3D-printed chest wall has been used for optimal surgical planning, namely determining the length, the shape the insertion points, and the number of bars required [13-19]. Despite the aid by computer, the design of the shape of the bar remained quite intuitive and empirical. Xie et al (2017) [18] used a computed tomography (CT) imaging database and selected a healthy person by age, sex, and thoracic transverse diameter to determine the shape of the bar. Kim at (2019) [19] used the CT scans of patients with PEx to design the desired shape of the bar by intuitively drawing the line of the ideal bar on the CT scan.

We propose a new CT-based computer-aided mathematical algorithm to determine the optimal shape of the Nuss bar and tested this technique virtually and clinically.

Material and Methods

Ethics Statement

A prospective patient study was approved by the Local Research Ethics Committee of the BAZ County and University Teaching Hospital, Miskolc, Hungary (#BORS-07/2021). The procedure was explained in detail, and informed consent was taken from the parents and patients.

Determination of the Normal Sterno-Vertebral Distance

The construction of the chest model was based on 2 patient groups. Group A consisted of 97 patients, all of whom had a depressive anterior chest wall deformity, specifically PEx. Group B consisted of 103 patients without PEx, and thus the patients were considered healthy in this regard. Patients of the same age range, 14 to 25 years (average 16.6 years), were selected for both patient groups.

CT images of patients with PEx (group A) served as the basis for the reconstruction model. Group A consisted of 13 female patients, age 14 to 19 (mean: 16.08 years), and 84 male patients, age 14 to 25 (mean: 16.25 years; **Table 1**).

Chest CT scans were acquired using a 128-slice Siemens Somatom Definition instrument in low-dose mode, without contrast material. Data analysis was performed using software written in the Python language, and modeling was run on a standard notebook computer. The software was platform independent, and worked with MS Windows, Linux, and Mac OS operating systems.

The patients in group A were initially examined, and from each CT scan, the slice depicting the deepest deformity was selected. Following this, in this group, the distance between the intermamillary line, which connects the nipples, and the deepest point of the deformity was determined. This approach was confirmed by the computed Haller index. The distance ranged from 0.9 to 4.8 cm, with an average of 2.98±0.98 cm (mean±SD).

Next, the geometry of a healthy chest was determined in group B. The chests of patients without deformity (group B) were examined at the same distance of 2.98 cm below the transverse breast line. To determine the baseline parameters of a healthy chest wall topography, the CT scans of chests without deformity in group B were used. Group B consisted of 103 patients, 42 of which were female, age 14 to 20 (mean: 17.31 years), and 61 were male, age 14 to 20 (mean: 17.15 years; **Table 2, Figures 1, 2**). For the selection of patients in group B, it was important that no traumatic injury or other chest wall malformation causing chest deformity was present. In these patients, the CT scan was taken for a different, unrelated illness. One

Indexed in: [Current Contents/Clinical Medicine] [SCI Expanded] [ISI Alerting System] [ISI Journals Master List] [Index Medicus/MEDLINE] [EMBASE/Excerpta Medica] [Chemical Abstracts/CAS]

Table 1. Data of patients (group A) with pectus excavatum.

Sex	n	Sagittalis diameter (cm)	Axial diameter (cm)	Age (yrs)	Haller index
Female	13	4.50-7.50 Mean: 6.08 SD: 0.86	21.50-25.00 Mean: 22.77 SD: 1.09	14-19 Mean: 16.08	3.13-5.44 Mean: 3.83 SD: 0.65
Male	84	3.00-12.00 Mean: 7.23 SD: 1.63	19.00-31.00 Mean: 24.78 SD: 2.18	14-25 Mean: 16.25	2.19-6.63 Mean: 3.59 SD: 0.83
Total	**97**	**3.00-12.00 Mean: 7.07 SD: 1.60**	**19.00-31.00 Mean: 24.51 SD: 2.18**	**14-25 Mean: 16.23**	**2.19-6.63 Mean: 3.62 SD: 0.81**

The table shows the sagittal and horizontal (axial) diameters of the chest, along with the resulting Haller index, for 97 patients in the pectus excavatum group, categorized by sex and age.

Table 2. Data of control group (group B) patients without chest wall malformation.

Sex	n	Sagittalis diameter (cm)	Axial diameter (cm)	Age (yrs)	Haller index
Female	42	7.50-12.00 Mean: 9.65 SD: 1.12	19.50-24.00 Mean: 21.76 SD: 1.84	14-20 Mean: 17.31	1.87-2.82 Mean: 2.28 SD: 0.25
Male	61	8.00-13.50 Mean: 10.51 SD: 1.39	18.00-26.70 Mean: 23.57 SD: 1.84	14-20 Mean: 17.15	1.5-3.13 Mean: 2.28 SD: 0.33
Total	**103**	**7.50-13.50 Mean: 10.16 SD: 1.35**	**18.00-26.70 Mean: 22.83 SD: 1.85**	**14-20 Mean: 17.21**	**1.50-3.13 Mean: 2.28 SD: 0.30**

The table presents the sagittal and horizontal (axial) diameters of the chest, as well as the resulting Haller index, for 103 patients in the group without pectus excavatum. The data are categorized by sex and age. The measurements were taken (based on the information obtained from the pectus excavatum group), 2.98 cm away from the transverse nipple line.

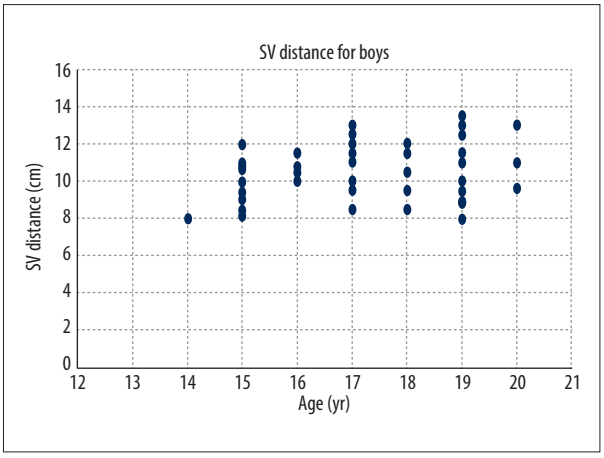

Figure 1. Sterno-vertebral distance nomogram of age in boys. Figure illustrates the distribution of the normal sterno-vertebral distance among the 103 patient of group B. No clear trend is visible.

Figure 2. Sterno-vertebral distance nomogram of age in girls. Figure illustrates the distribution of the normal sterno-vertebral distance among the 103 patient of group B. No clear trend is visible.

Indexed in: [Current Contents/Clinical Medicine] [SCI Expanded] [ISI Alerting System] [ISI Journals Master List] [Index Medicus/MEDLINE] [EMBASE/Excerpta Medica] [Chemical Abstracts/CAS]

Table 3. Classification and explanation of Haller index in pectus excavatum.

Degree of pectus excavatum	Range of Haller Index
Normal	2-2.5
Mild excavatum	2.6-3.2
Moderate excavatum	3.2-3.5
Severe excavatum	3.5

$$\text{Haller index} = \frac{\text{thorax horizontal diameter}}{\text{thorax sagitalis diameter}}$$

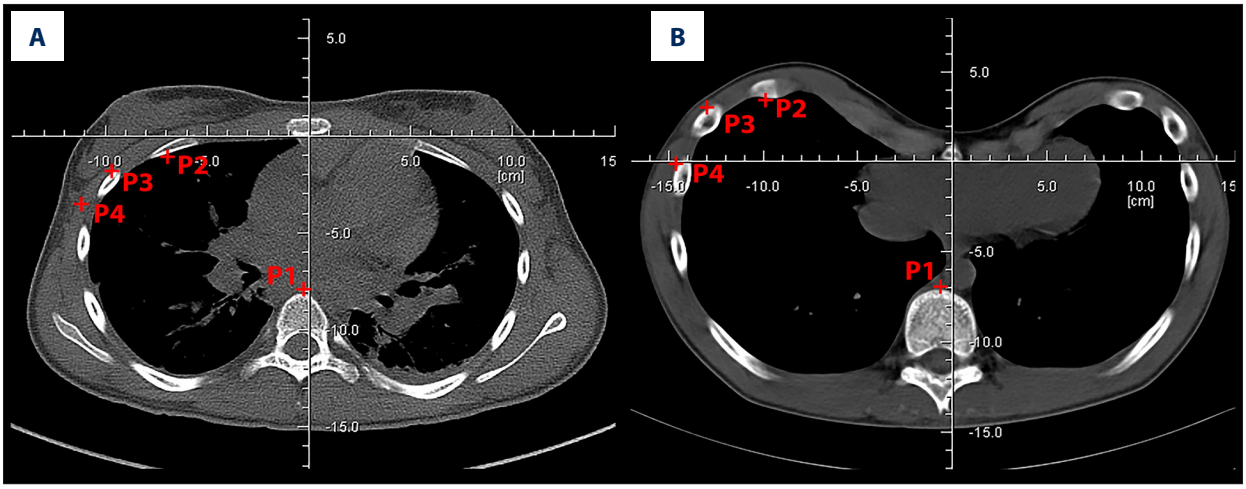

Figure 3. (**A, B**) P1-P4 reference points for patients in groups A and B. The image illustrates reference points, necessary for the bar construction, showing them in cases without chest deformity and with chest deformity. The points do not participate in the correction during the shape transformation, they remain constant. *The software used for figure creation was Phyton.*

key element was to identify the sterno-vertebral distance in the healthy population to develop the algorithm.

The classification and explanation of the Haller index in PEx is shown in **Table 3**, with the Haller index=thoracic horizontal diameter/thoracic sagittal diameter.

Computer-Aided Design of the Custom-Made Nuss Bar and Virtual Correction of PEx

The coordinate system of CT scans was provided by Siemens Singovia CT version 2012B software. The intersection of the X- and Y-axes were at the center of the intrathoracic surface of the sternum. The X-axis was parallel to the surface of the CT examining table. The center of the intrathoracic arc of the vertebral body in the scan was used as the mathematical origin required for the geometric editing. The reason for this choice of origin was that this point did not move during the correction of the PEx deformation.

The algorithm for the software development was created via the following main steps:

1. For the CT scan to be suitable for computer modelling, the ribs and vertebrae must be clearly visible without respiratory and other artifacts. Additionally, the deepest point of the chest deformity and the cross section of the associated ribs need to be clearly visible.
2. The magnification was standardized, and the images were uniformly enlarged/decreased to a resolution of 30 pixels/cm.
3. Construction of the bar was done on the CT scan that showed the deepest deformity of the chest. The algorithm used fixed points that were not part of the deformity, and these points did not change/move during the correction.

- Point P1 was placed at the center of the anterior curve of the vertebral body in front of the deepest point of the deformity. It could be identified automatically, via image analysis.
- Point P2 lies at the edge of the deformity, where the bar exits the chest cavity during correction.
- Point P3 was placed at the surface where the bar, after the exit, first makes contact with the rib on the external chest wall. The current positions of P2 and P3 are always determined by the deformity.
- Point P4 indicates the end of the bar, positioned between the anterior and mid-axillary lines. Locating P4 is somewhat intuitive, as it marks the end of the bar, requiring some practice (**Figure 3A, 3B**).

Indexed in: [Current Contents/Clinical Medicine] [SCI Expanded] [ISI Alerting System] [ISI Journals Master List] [Index Medicus/MEDLINE] [EMBASE/Excerpta Medica] [Chemical Abstracts/CAS]

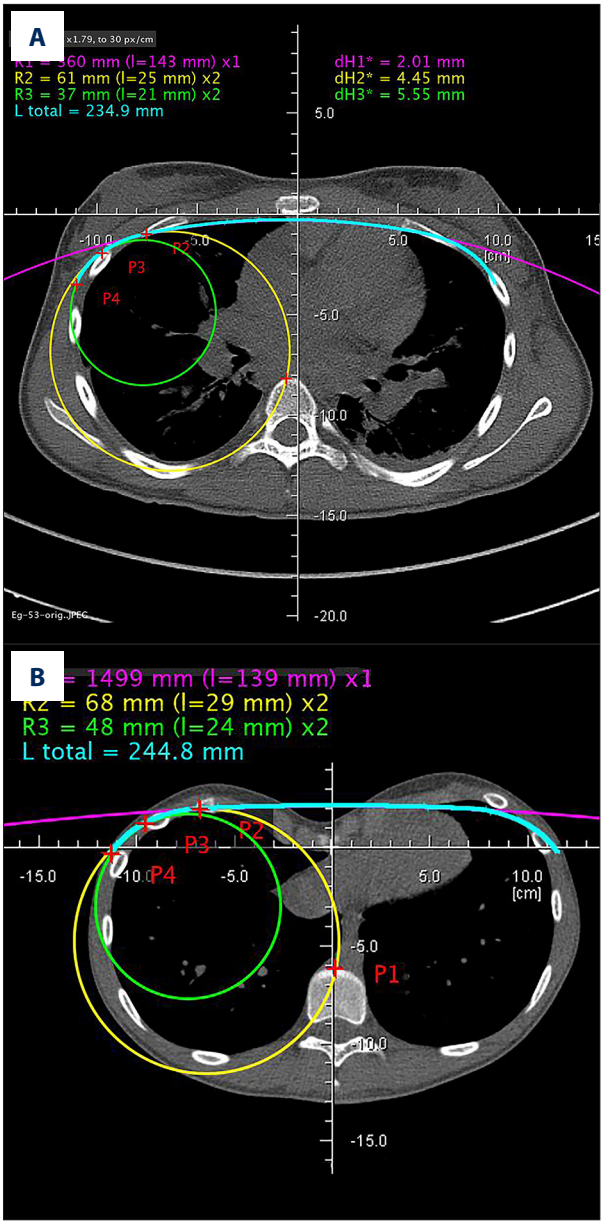

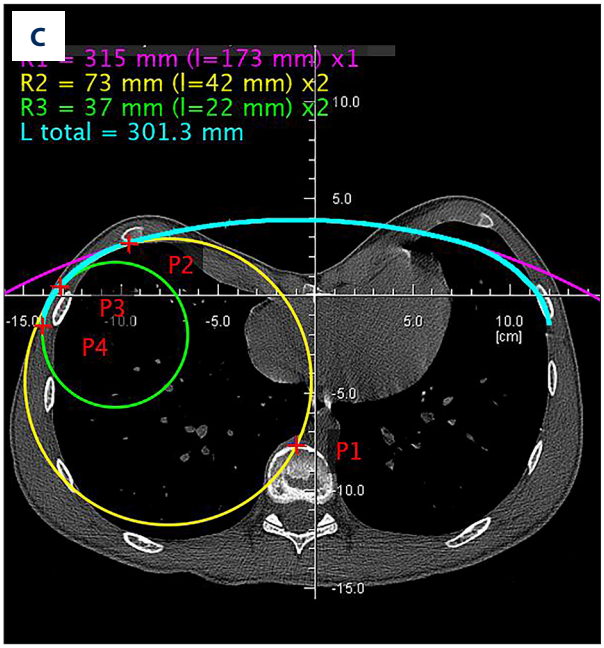

Figure 4. Virtual correction with MATLAB R2020a software. (**A**) No deformity, intact chest; (**B**) pectus excavatum deformed symmetrical chest; and (**C**) asymmetrical chest. The application can be used both for symmetrical and asymmetrical shapes. This is a mathematical model for correcting chest deformities. The images show the circles connecting the reference points, touching each other and thus drawing the shape of the bar. *The software used for figure creation was Phyton.*

The algorithm presented here is based on 3 matching circular arches. The 3 circles are marked by their color.

- The yellow circle is defined by P1, P2, and P3. The resulting circle radius is R2.
- The green circle passes through P3 and P4, as well as touching the yellow circle at P3 (note that touching circles have the same tangent at the touching point; therefore, their centers and P3 lie on the same line). The green circle has radius R3.
- Finally, a purple circle is determined by P2 and its Y-axis symmetrical point, denoted as P2'. This circle touches the yellow circle, and its center lies on the Y-axis. The purple circle has radius R1.

4. The final shape is a line (thick turquoise color) that is seamlessly composed of 3 arc segments:
- From P4 to P3 it follows the green circle, over length L3.
- From P3 to P2, it follows the yellow circle over length L2.
- From P2 it follows the purple one until it symmetrically crosses the Y-axis, over length L1.
- The implant is designed to be symmetric to the Y-axis, and at the junction points the tangent of the connecting arcs is the same; therefore, the shape is smooth along the full path (**Figure 3A, 3B**).

Based on our practice, the bar, after exiting the thorax, must lean on at least 2 ribs so that the load can be distributed. The construction of the shape should be performed strictly on the bone structure without considering any soft tissues.

5. The bent Nuss bar is intended to be symmetrical. Symmetry refers to the vertical axis (Y-axis) going through P1. The shape and the length of the bar determined by the P2-P2, P2-P3, and P3-P4 sections, which are defined by circular arcs of different radii. These are seamlessly connected to each other, resulting in an equal tangent of connected arcs (**Figure 4A-4C**).

Indexed in: [Current Contents/Clinical Medicine] [SCI Expanded] [ISI Alerting System] [ISI Journals Master List] [Index Medicus/MEDLINE] [EMBASE/Excerpta Medica] [Chemical Abstracts/CAS]

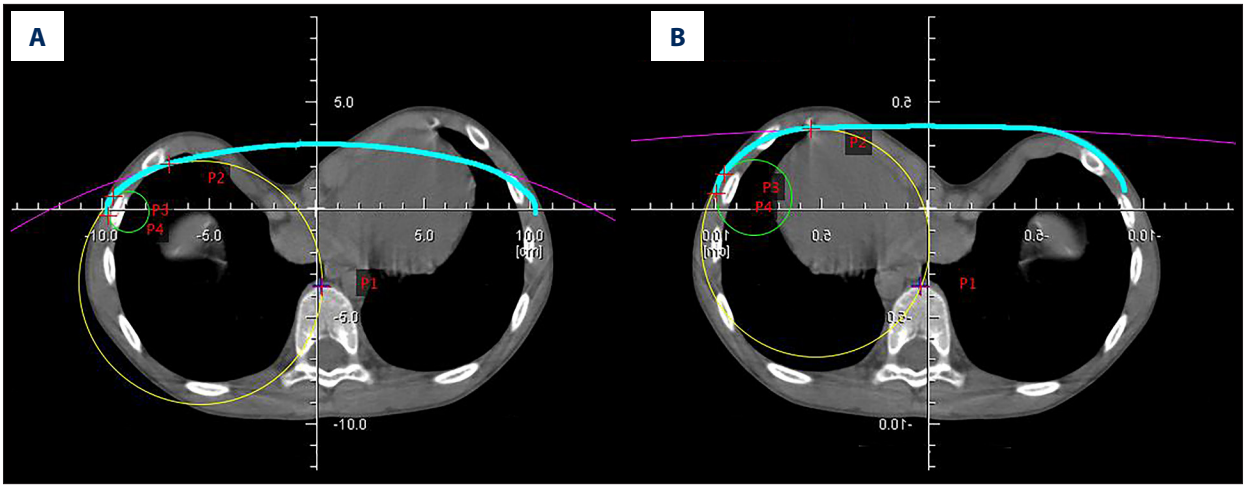

Figure 5. Planning in asymmetry. (**A**) Asymmetry in a CT scan of a patients with pectus excavatum; (**B**) mirrored scan of (**A**). The model can be used in cases of asymmetrical deformities as well. The software can perform the construction from the radiological right side, as in the images from the left side. In cases of asymmetry, the construction begins from the more favorable chest shape. If necessary, the software can mirror the image along the Y-axis. *The software used for figure creation was Phyton.*

Thus, the curvature of the bar is characterized by 3 radii (R1, R2, and R3) and 3 arc lengths (L1, L2, and L3). The joining of the arcs is smooth because the circles touch each other. L1 represents the length between P2 and the Y-axis. L2 denotes the length between P2 and P3 along the curve. Similarly, L3 refers to the length between P3 and P4.

The total length of the bar is given by L=2×(L1+L2+L3). The value is automatically displayed on the CT image after editing.

The human body is mostly symmetrical; therefore, this is what we took as a basis. In the case of near or complete symmetry, the editing starting point was the right side of the body, which corresponded to the left side of the image.

The algorithm can also be used in the case of an asymmetric chest. In this case, the more contoured, less distorted half of the chest can be taken as a basis. **Figure 5A and 5B** illustrate this model.

The construction starts on the less deformed side and draws the curve on the other side as well. The algorithm can start the selection of points on the left side, so if the opposite side is the right side, then the image must be mirrored for editing. This does not take anything away from the accuracy of the construction but is just a technical requirement of the software. Asymmetric bars in the lateral direction (perpendicular to the normal force vector of the sternum) always include a load that can destabilize the implant, leading to slipping. To avoid this, we did not use asymmetric bars. Of course, in very rare cases with marked deformations, individual solutions can be required, and our methodology may not be applicable.

Virtual Correction of PEx

We performed virtual correction on the CT scans of 60 patients with PEx, using the image depicting the deepest deformity. Following the correction, we measured the sterno-vertebral distance and compared it with the data from the healthy population (group B, **Table 2, Figures 1, 2**).

Statistical Analysis

The mean±standard deviation (SD) of the normal and the virtually corrected the sterno-vertebral distance was compared with the Mann-Whitney U test. The *P* value was set on 0.05.

Bending of the Nuss Bar

Straight unisex 3-mm thick bars made out of medical-grade stainless steel (SS317 alloys of 18% Cr, 15% Ni, 3% Mo, and 1.6% Mn) manufactured by Sanametal Ltd (Eger, Hungary) were used in the study. The shape of the virtual bar produced by the algorithm was printed on paper in life size (A3 in 1: 1 scale) and was used as a guide to generate the required shape using hand bending tools. Two manual metal (Aesculap) bending pliers were used to bend the steel bars to the desired shape, and then the bars were sterilized.

Clinical Pilot Trial

Ten modified Nuss procedures were performed following prior patient information and consent (8 boys and 2 girls, age of 16.8±2.6 years (mean±SD). The group included 4 symmetrical and 6 moderately asymmetrical cases of PEx. We assessed the outcome of the surgery outcome by recording the satisfaction of the patient and surgeon on a 1 to 10 scale.

Indexed in: [Current Contents/Clinical Medicine] [SCI Expanded] [ISI Alerting System] [ISI Journals Master List] [Index Medicus/MEDLINE] [EMBASE/Excerpta Medica] [Chemical Abstracts/CAS]

Results

Determination of the Normal Sterno-Vertebral Distance

In the PEx patient group, the deepest point of the deformation was found at 0.9 to 4.8 cm (2.98±0.98 cm mean±SD) below the intermammillary line. At this position, the healthy group exhibited a sterno-vertebral distance of 8.0 to 13.5 cm (10.51±1.39 mean±SD) for boys and 7.5 to 12.0 cm (9.65±1.12 mean±SD) for girls (**Figures 1, 2**).

Computer-Aided Design of the Custom-Made Nuss Bar and Virtual Correction PEx

The average sterno-vertebral distance in PEx patients after the correction was 7.5 to 13 cm (10.28±1.27 mean±SD) for a group of girls and boys.

Statistical Analysis

The chest parameters of healthy children and those who underwent surgery did not follow a normal distribution; hence, we conducted a non-parametric test. The result of the Mann-Whitney U test at 5% significance level was P=0.44. The median and interquartile values for the 2 groups were as follows: healthy group 10.0 (9.15-11), and post-surgery group 10.5 (9.5-11.25). The difference between the healthy group without deformities and the post-surgery corrective group was not significant; that is, there was no statistical difference in the medians. Our procedure yielded results postoperatively that closely resembled the shape of a chest without deformity. The calculations were performed using the R statistical programming package (**Figure 6**).

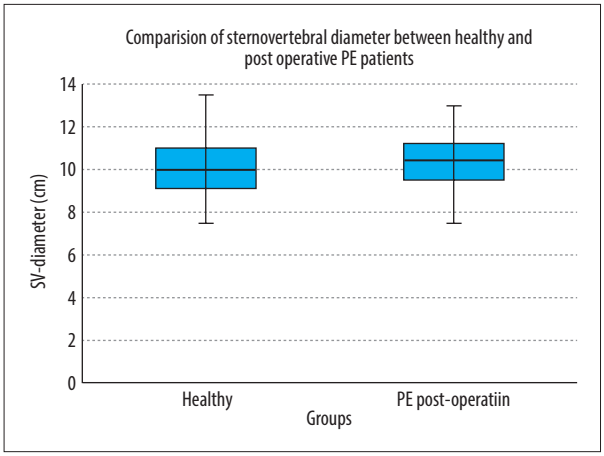

Figure 6. Statistical comparison based on the sterno-vertebral distance measurement between the post-reconstruction state after pectus excavatum corrective virtual surgery and the group of patients without deformities. The reconstructive surgery's effectiveness was statistically validated.

Bending of the Nuss Bar

The premanufactured bars were seamless, free from any irregularity.

Clinical Pilot Trial

The custom made bars were successfully implanted without the need of further bending or alteration. The operation time was significantly shorter. The postoperative patient and surgeon's satisfaction scores were 9.5 and 9.2 out of 10, respectively (**Table 4**).

Table 4. Pilot study data of patients operated on with pectus excavatum.

Patient number	1	2	3	4	5	6	7	8	9	10
Sex	Male	Male	Male	Male	Male	Male	Male	Male	Female	Female
Age	17	15	15	17	15	15	16	16	18	15
Haller index	4.2	7.14	5.00	3.3	5.6	3.4	4.2	3.4	4.2	5.6
Number of bars	1	2	1	1	2	1	1	1	1	2
Patient satisfaction score (1-10)/10	10	8	10	9	10	10	9	10	9	10
Surgeon satisfaction score (1-10)/10	9	8	10	10	8	10	9	8	10	10
Operation time (min)	75	145	80	75	90	60	105	155	80	95
Stay in hospital (day)	6	6	5	6	6	6	6	7	7	5

The table shows data from patients operated on using the technique described by the authors. It is a heterogeneous group with varying Haller indices. The first bar was customized for each individual, while the shaping of the second bar was possible only after the first implantation. Dynamic chest model is currently unavailable; therefore, we could design the first bar tailored only to the individual. Satisfaction is a subjective factor from both the patient and surgeon perspectives. Comparing results is challenging due to the unique nature of each deformity. The surgery duration is shortened, as the bar bending is not done beside the operating table.

Indexed in: [Current Contents/Clinical Medicine] [SCI Expanded] [ISI Alerting System] [ISI Journals Master List] [Index Medicus/MEDLINE] [EMBASE/Excerpta Medica] [Chemical Abstracts/CAS]

Discussion

Our results suggest that our algorithm-driven software can calculate the optimal geometry of the bar based on the CT images, as the virtually corrected sterno-vertebral distances of PEx patients fell within the normal range. The method does not require high computational resources; a mid-range desktop or portable computer is sufficient for the necessary analysis.

When designing the program, we did not use the Haller index as a reference, but rather the data from healthy patients. The rationale behind this is that we believe the Haller index is not sufficiently accurate. Patients' body types can range from normal to asthenic or pyknic. In an unpublished study, we categorized a significant number of patients without PEx based on the Haller index. According to this, 75% were classified as having pectus carinatum, 4% as pectus excavatum, while only 11% were found to be normal.

The discretion of the surgeon is not entirely excluded from our method, as it is necessary for surgeons to determine the reference points P1-P4, upon which the algorithm can build to shape the ideal chest; however, these reference points are clearly well defined. We believe that, in this way, a more accurate result can be provided than by the previously published methods.

A clear advantage of our proposed system is that the length of the bar is obtained from the lengths of the arcs drawn on the ribcage on the CT image and not from a manual measurement on the patient's chest, where variable amount of soft tissue, namely muscle or fat, are usually measured. We found all pre-bent bars precisely fit the patient's chest deformity during surgery.

In 1 patient who underwent successful surgery for a PEx before the launch of the present study, a CT scan was performed for another reason. The shape and placement of the bar on the CT matched the one we planned virtually for this patient, based on his preoperative CT scan (**Figure 7**). The fact that none of the pre-designed bars needed to be removed for further correction after the initial implantation was very reassuring. Because the insertion of the bar itself poses the highest risk of severe complications, such as cardiac injury or severe bleeding, we can state that the pre-designed bar increases the safety of the procedure.

In our experience, asymmetric PEx bars are known to be exposed to lateral forces and are generally less stable, meaning there is higher risk of bar migration. To prevent bar migration, we generally avoid the use of asymmetric bars, even in cases of significant asymmetric deformities; therefore, our method is suitable for these cases as well.

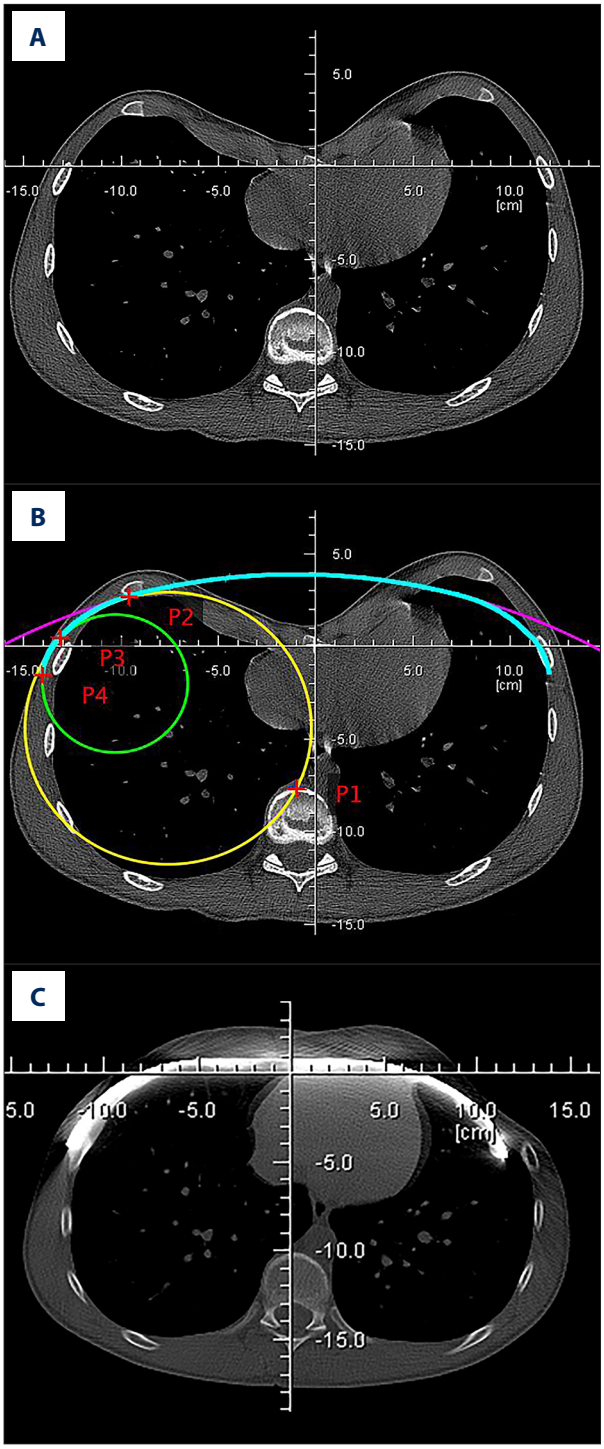

Figure 7. (**A**) Preoperative, (**B**) virtually planned, and (**C**) postoperative computed tomography scan of a patient. The patient was operated by the lead author. The first image shows the chest deformity. The second image displays the virtually edited shape and appropriate length of the bar. The third image shows the postoperative condition. The examination was conducted for another medical condition. *The software used for figure creation was Phyton.*

Indexed in: [Current Contents/Clinical Medicine] [SCI Expanded] [ISI Alerting System] [ISI Journals Master List] [Index Medicus/MEDLINE] [EMBASE/Excerpta Medica] [Chemical Abstracts/CAS]

Altogether, the patient and surgeon satisfaction scores were very high, although we acknowledge that satisfaction is a subjective parameter.

Preoperative planning, bending, checking, and sterilization can require some effort and time, but this pays off with shorter surgical times, optimal results, and increased safety.

We noticed slight distortion on CT scans in cases when the patient did not lie straight on the table during the scan. However, these patients were quite cooperative, and their preparation was generally sufficient to avoid artefact and incorrect bar planning. Furthermore, minor distortions could be corrected by the software, adjusting the image left or right to achieve a horizontal position.

Limitations

We acknowledge the determination of the shape of the bar is only one starting element of modern surgical planning. Finite element analysis and simulated surgery on 3D-printed models are also important tools and can be combined with our methods. In our clinical trial, we did not use these methods; however, we achieved very promising results. At selection of the site of bar insertion, we relied on our previous experience and always selected the point of the deepest deformity. We were also not able to predict the need for a second bar. However, in our pilot study, only 30% of cases required insertion of a second bar.

Conclusions

The shape of the pectus bar and its fit to the thorax are key factors of a successful surgery. In the era of personalized medicine and patient-tailored therapy, the correction requires meticulous design from the engineers and matching precision from the surgeons. We developed a simple, safe, and cost-effective method for the computation of the bar shape. The designed bars were successfully prepared and tested, and the effectiveness of the reconstructive surgery could be statistically validated.

We believe our new algorithm can be useful alone or combined with the abovementioned tools for surgical planning to further improve preoperative planning of the Nuss procedure.

Acknowledgements

We would like to thank Prof. Dr. Balázs Gereben DSc (Institute of Experimental Medicine, Budapest, Hungary) for critical reading of the manuscript. The authors appreciate the support of Borsod-Abaúj-Zemplén County Hospital and University Teaching Hospital (BKEOK), Department of Pediatric Surgery, Traumatology and Burns, Miskolc, Hungary, especially that of Dr. Ákos L. Kiss, senior Head of Department. The authors are also grateful to Orsolya Lukács for her help with the preparation of the graphical abstract and Gabriel T. Kardos (MBA) for assistance in editing this work.

Ethical Statement

The study was approved by the Local Research Ethics Committee under the number BORS-07/2021, BAZ County and University Teaching Hospital, Miskolc, Hungary.

Department and Institution Where Work Was Done

This work was performed at the Department of Pediatric Surgery, Traumatology and Burns, Borsod-Abaúj-Zemplén County Hospital and University Teaching Hospital (BKEOK), Miskolc, Hungary.

Declaration of Figures' Authenticity

All figures submitted have been created by the authors who confirm that the images are original with no duplication and have not been previously published in whole or in part.

References:

1. Haller JA Jr., Kramer SS, Lietman SA. Use of CT scans in selection of patients for pectus excavatum surgery: A preliminary report. J Pediatr Surg. 1987;22(10):904-6
2. de Loos ER, Höppener PF, Busari JO, et al: [Pectus excavatum: Not just a cosmetic problem.] Ned Tijdschr Geneeskd. 2020; 164:D4509 [in Dutch]
3. Fortmann C, Petersen C. Surgery for deformities of the thoracic wall: No more than strengthening the patient's self-esteem? Eur J Pediatr Surg. 2018;28(4):355-60
4. Abdullah F, Harris J. Pectus excavatum: More than a matter of aesthetics. J Pediatr Ann. 2016;45(11):e403-e6
5. Beiser GD, Epstein SE, Stampfer M, et al. Impairment of cardiac function in patients with pectus excavatum, with improvement after operative correction, N Engl J Med. 1972;287(6):267-72
6. Jaroszewski DE. Pectus excavatum Not just a cosmetic concern. Mayo Clinic Cardiovascular Oct, 2017. Available from: https://www.mayoclinic.org/medical-rofessionals/cardiovascular-diseases/news/pectus-excavatum-not-just-a-cosmetic-concern/mac-20430716
7. Haecker FM, Sesia S. Non-surgical treatment of pectus excavatum. J Vis Surg. 2016;2:63
8. Nuss D, Kelly RE Jr., Croitoru DP, Swoveland B. Repair of pectus excavatum. Pediatric Endosurgery & Innovative Techniques. 1998;4:205-21
9. Nuss D, Kelly RE Jr., Croitoru DP, Katz ME. A 10-year review of a minimally invasive technique for the correction of pectus excavatum. J Pediatr Surg. 1998;33(4):545-52
10. Ravitch MM. The operative treatment of pectus excavatum. Ann Surg. 1949;129(4):429-44

Indexed in: [Current Contents/Clinical Medicine] [SCI Expanded] [ISI Alerting System] [ISI Journals Master List] [Index Medicus/MEDLINE] [EMBASE/Excerpta Medica] [Chemical Abstracts/CAS]

11. Bardají C, Cassou L. Taulinoplasty: the traction technique – a new extrathoracic repair for pectus excavatum Ann Cardiothorac Surg. 2016;5(5):519-22
12. Frediani S, Beati F, Pardi V, et al. Case report: Modified taulinoplasty: A new technique for minimally invasive repair of pectus excavatum. Front Surg. 2023;10:1343515
13. Vilaça JL, Rodrigues PL, Soares TR, et al. Automatic prebent customized prosthesis for pectus excavatum minimally invasive surgery correction. Surg Innov. 2014;21:290-96
14. Bellia-Munzon G, Martinez J, Toselli L, et al. From bench to bedside: 3D reconstruction and printing as a valuable tool for the chest wall surgeon. J Pediatr Surg. 2020;55(12):2703-9
15. Gaspar Pérez M, Núñez García B, Álvarez García N, et al. Initial experience with 3D printing in the use of customized Nuss bars in pectus excavatum surgery. Cir Pediatr. 2021;34(4)186-90
16. Matsuo N, Matsumoto K, Taura Y, et al. Initial experience with a 3D printed model for preoperative simulation of the Nuss procedure for pectus excavatum. J Thorac Dis. 2018;10:E120-24
17. Wang L, Guo T, Zhang H, et al. Three-dimensional printing flexible models: A novel technique for Nuss procedure planning of pectus excavatum repair. Ann Transl Med. 2020;8:110
18. Xie L, Cai S, Xie L, et al. Development of a computer-aided design and finite-element analysis combined method for customized Nuss bar in pectus excavatum surgery. Sci Rep. 2017;7(1):3543
19. Kim YJ, Heo JY, Hong KH, et al. Computer-aided design and manufacturing technology for identification of optimal nuss procedure and fabrication of patient-specific nuss bar for minimally invasive surgery of pectus excavatum. Appl Sci. 2019;9(1):42

Indexed in: [Current Contents/Clinical Medicine] [SCI Expanded] [ISI Alerting System] [ISI Journals Master List] [Index Medicus/MEDLINE] [EMBASE/Excerpta Medica] [Chemical Abstracts/CAS]